

W-shaped 1,3-Di(2,4-dicarboxyphenyl)benzene Based Lanthanide Coordination Polymers with Tunable White Light Emission

Liming Fan,^{a,c} Weiliu Fan,^a Bin Li,^b Xian Zhao^{*a} and Xiutang Zhang^{*a,b}

Received (in XXX, XXX) Xth XXXXXXXXX 2016, Accepted Xth XXXXXXXXX 2016

DOI: 10.1039/c6nj00000x

ABSTRACT: Series of trinuclear coordination polymers (CPs), $\{[Ln_{1.5}(DDB)(FA)_{0.5}(H_2O)_{2.5}] \cdot 6H_2O\}_n$ (Ln = Sm for **1**, Eu for **2**, Tb for **3**, Dy for **4**), have been constructed from Ln cations and 1,3-di(2,4-dicarboxyphenyl)benzene (H₄DDB) with the help of the *in situ* generation of formate anions under solvothermal reactions. Their structures have been determined by single-crystal X-ray diffraction analyses and further characterized by elemental analyses, IR spectra, powder X-ray diffraction (PXRD), and thermogravimetric (TG) analyses. Complexes of **1–4** exhibit the unprecedented (3,8)-connected 3D architectures with the Schlafli Symbol of $(4.5^2)_2(4^2.5^{12}.6^6.7^5.8^3)$, based on the trinuclear $[Ln_3(COO)_6]$ SBUs. Besides, luminescence investigation indicating that **1** and **4** show ligand-based fluorescence, while **2** and **3** show typical red or green emission with 4f–4f transitions for Ln ions. White light emission can be achieved by doping the Dy ions into the Eu complex.

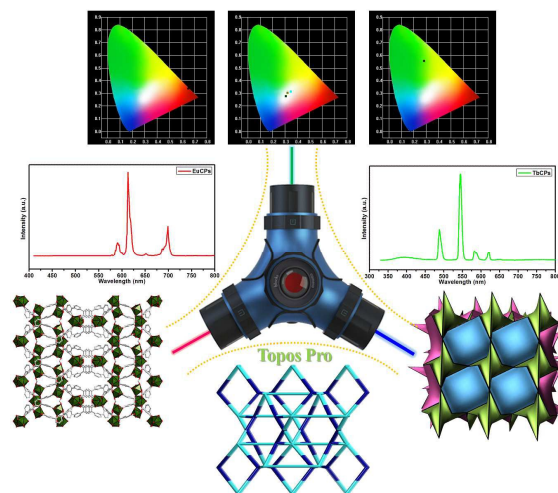
Introduction

The lanthanide coordination polymers (LnCPs), an emerging class of functional crystalline materials, have attracted much attention for their fascinating structures and interesting topologies, as well as their potential applications in luminescence, magnetic, gas storage and separation, drug delivery, and sensing for their well-shielded 4f configuration.^{1–3} Although numerous LnCPs with fascinating structural diversities and novel topologies have been obtained, the rational design of those materials is still a arduous and remarkable marathon challenge due to the high coordination number and flexible coordination geometry of lanthanide ions, as well as the structural characteristics of the organic linkers.⁴

Lanthanide ions based CPs have unique advantages over other traditional CPs with regard to functional luminescence features, for the f–f transitions of lanthanide ions endow the LnCPs narrow bandwidth, high luminescence quantum yield, long lived emission, wide emission bands cover the visible and infrared parts of the optical spectrum as well as the large Stokes shift.^{5,6} In addition, the introduction of organic ligands attaching the Ln^{III} ions expanded the domain of these luminescent materials. Taking the organic linkers and inorganic units into consideration, LnCPs provide special platforms for these functional materials.⁷

Recently, many polycarboxylates have been introduced into the LnCPs by either ligand design or substituent

modification.⁸ However, most of these LnCPs are designed rather randomly and lack systematic comparison, which would be helpful to understanding crystal growth and structure–property relationships.^{9–11} Previous research on LnCPs assemblies using 3,3',5,5'-biphenyltetracarboxylic acid (H₄BPT) and 4,5-di(4'-carboxylphenyl)phthalic acid (H₄DPT) states a reliable strategy for obtaining new topological prototypes of coordination nets.^{11a} Also, a minor change of the carboxylate building blocks may be applied to realize good structural control of the resulting CPs. Thus, these considerations inspired us to explore novel LnCPs with the selected W-shaped 1,3-di(2,4-dicarboxyphenyl)benzene (H₄DDB). Herein, we reported the syntheses and characterizations of series isomorphous coordination polymers, $\{[Ln_{1.5}(DDB)(FA)_{0.5}(H_2O)_{2.5}] \cdot 6H_2O\}_n$ (Ln = Sm for **1**, Eu for **2**, Tb for **3**, and Dy for **4**) (Scheme 1). The four LnCPs exhibited trinuclear $[Ln_3(COO)_6]$ SBUs based 3D (3,8)-connected $(4.5^2)_2(4^2.5^{12}.6^6.7^5.8^3)$ architectures.



Scheme 1. The structures, properties, and applications of titled LnCPs.

^a State Key Laboratory of Crystal Materials, Shandong University, Jinan 250100, China. E-mail: xianzhao@sdu.edu.cn.

^b Advanced Material Institute of Research, College of Chemistry and Chemical Engineering, Qilu Normal University, Jinan, 250013, China. E-mail: xiutangzhang@163.com.

^c Department of Chemistry, College of Science, North University of China, Taiyuan 030051, China.

†Electronic Supplementary Information (ESI) available: powder X-ray diffraction (PXRD) patterns, thermogravimetric analysis (TGA) and IR spectra for **1–4**. X-ray crystallographic data, CCDC 1442620–1442623 for **1–4**. See DOI:10.1039/c6nj00000x.

Experimental Section

Materials and Physical Measurements. All chemicals were purchased from Jinan Henghua Sci. & Tec. Co. Ltd. without further purification. IR spectra were measured on a NEXUS 670 FTIR spectrometer at the range of 600–4000 cm^{-1} . Elemental analyses were carried out on a CE instruments EA 1110 elemental analyzer. Thermogravimetric analyses (TGA) were performed under air condition from room temperature to 800 $^{\circ}\text{C}$ with a heating rate of 10 $^{\circ}\text{C min}^{-1}$ on Perkin–Elmer TGA–7 thermogravimetric analyzer. X–ray powder diffractions were measured on a Panalytical X–Pert pro diffractometer with Cu– $K\alpha$ radiation. Fluorescence spectra were recorded for the solid samples on an F–4600 FL spectrophotometer equipped with a 150 W xenon lamp as an excitation source at room temperature. The CIE (Commission Internationale de l'Eclairage) color coordinates were calculated on the basis of the international CIE standards.

Synthesis of $\{[\text{Ln}_{1.5}(\text{DDB})(\text{FA})_{0.5}(\text{H}_2\text{O})_{2.5}]\cdot 6\text{H}_2\text{O}\}_n$ ($\text{Ln} = \text{Sm}$ for **1, **Eu** for **2**, **Tb** for **3**, and **Dy** for **4**).** A mixture of H_4DDB (0.15 mmol, 0.066 g), $\text{Ln}(\text{NO}_3)_3\cdot 6\text{H}_2\text{O}$ (0.20 mmol, 0.092 g), NaOH (0.60 mmol, 0.024 g), 8 mL H_2O , and 2 mL DMF was placed in a Teflon–lined stainless steel vessel, heated to 170 $^{\circ}\text{C}$ for 5 days, followed by slow cooling (about 10 $^{\circ}\text{C/h}$) to room temperature. The colorless shuttle shaped block crystals of **1** were obtained. Yield of 54 % (based on Sm). Anal. (%) calcd. for $\text{C}_{45}\text{H}_{55}\text{O}_{35}\text{Sm}_3$ (1606.97): C, 33.63; H, 3.45. Found: C, 33.62; H, 3.63. IR (KBr pellet, cm^{-1}): 3343 (s), 1660 (m), 1568 (vs), 1526 (s), 1463 (m), 1398 (vs), 1100 (m), 780 (s), 692 (w). For **2**, the Yield of 54 % (based on Eu). Anal. (%) calcd. for $\text{C}_{45}\text{H}_{55}\text{O}_{35}\text{Eu}_3$ (1611.77): C, 33.53; H, 3.44. Found: C, 33.50; H, 3.61. IR (KBr pellet, cm^{-1}): 3364 (s), 1571 (vs), 1530 (s), 1471 (m), 1448 (m), 1405 (vs), 1180 (w), 1104 (w), 1011 (w), 781 (m), 694 (w). For **3**, the Yield of 54 % (based on Tb). Anal. (%) calcd. for $\text{C}_{45}\text{H}_{55}\text{O}_{35}\text{Tb}_3$ (1632.65): C, 33.10; H, 3.40. Found: C, 33.14; H, 3.47. IR (KBr pellet, cm^{-1}): 3332 (s), 1660 (m), 1573 (vs), 1533 (s), 1464 (s), 1402 (vs), 1178 (w), 1100 (w), 780 (m), 693 (w). For **4**, the Yield of 59 % (based on Sm). Anal. (%) calcd. for $\text{C}_{45}\text{H}_{55}\text{Dy}_3\text{O}_{35}$ (1643.39): C, 32.89; H, 3.37. Found: C, 32.24; H, 3.69. IR (KBr pellet, cm^{-1}): 3388 (s), 2933 (m), 1807 (w), 1769 (w), 1657 (m), 1566 (s), 1520 (s), 1491 (s), 1440 (m), 1395 (vs), 1102 (m), 781 (m), 694 (m).

X–ray Crystallography. Intensity data collection was carried out on a Siemens SMART diffractometer equipped with a CCD detector using Mo– $K\alpha$ monochromatized radiation ($\lambda = 0.71073$ Å) at 296(2) or 293(2) K. The absorption correction was based on multiple and symmetry–equivalent reflections in the data set using the SADABS program based on the method of Blessing. The structures were solved by direct methods and refined by full–matrix least–squares using the SHELXTL package.¹² There are some solvent accessible void volumes in the crystals of **1–4** which are occupied by highly disordered water molecules. The SQUEEZE procedure was applied to eliminate the disordered water molecules of **1–4**, and then the new files were generated. The water molecules for **1–4** are tentatively assigned based on TGA, elemental analysis as well as the SQUEEZE results. All non–hydrogen atoms were refined anisotropically. Hydrogen atoms were generated geometrically with fixed isotropic thermal

parameters. For **1–3**, the H atoms attached the coordinated water molecules are omitted for concise. For complex **4**, the hydrogen atoms (H12B and H12C) attached the coordinated water molecule (O12) are disordered and were refined with an occupancy ratio of 50:50. Crystallographic data for complexes **1–4** are given in Table 1. Selected bond lengths and angles for **1–4** are listed in Table S1. For complexes of **1–4**, further details on the crystal structure investigations can be obtained from the Cambridge Crystallographic Data Centre by visiting the website of <http://www.ccdc.cam.ac.uk/deposit>, on quoting the depository number CCDC–1442623 for **1**, 1442620 for **2**, 1442621 for **3**, and 1442622 for **4**, respectively.

Result and Discussion

General Characterization. Complexes **1–4** were obtained of H_4DDB and related lanthanide salts with the help of the *in situ* generation formate ions from the DMF molecules under the solvothermal reactions. They are stable in the air and have poor solubility in water and common organic solvents but can be slightly soluble in very high polarity solvents, such as DMF and DMSO. Powder X–ray diffraction (PXRD) has been used to check the phase purity of the bulk samples in the solid state. For complexes **1–4**, the measured PXRD patterns closely match the simulated patterns generated from the results of single crystal diffraction data, indicative of pure products (Fig. S1, see Supporting Information). The absorption bands around 3400 cm^{-1} for **1–4** can be attributed to the characteristic peaks of O–H vibrations. The vibrations at ca. 1500 and 1610 cm^{-1} correspond to the asymmetric and symmetric stretching vibrations of the carboxyl groups, respectively (Fig. S2).¹³

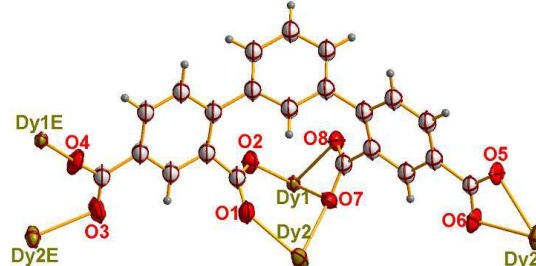


Figure 1. The coordination mode of H_4DDB in the formation of the **DyCP** (Symmetry codes: E: $y, -x, 1-z$; G: $1/2-x, y, 3/4-z$).

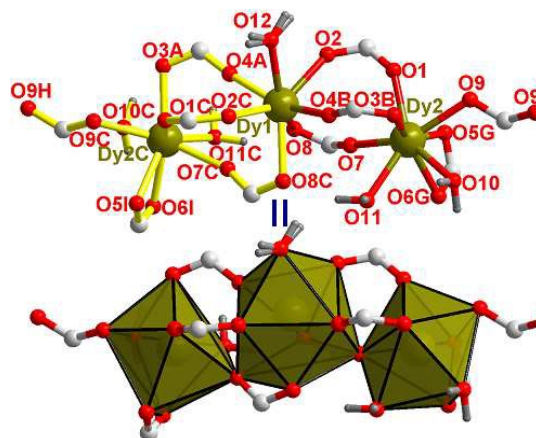
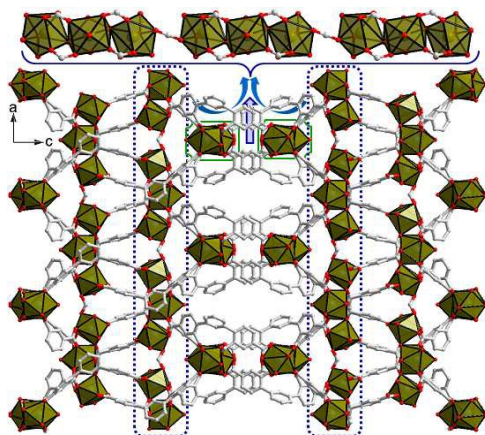
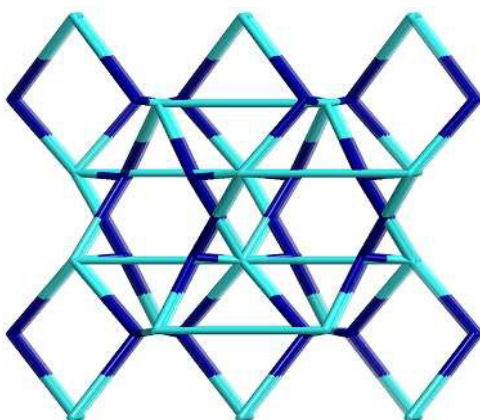


Figure 2. The trinuclear $[\text{Dy}_3(\text{COO})_6]$ SBUs (Symmetry codes: A: $1+x, -y, 1-z$; B: $-y, x, 1-z$; C: $1-x, -y, z$; F: $-x, -y, z$; G: $1/2-x, y, 3/4-z$; H: $1+x, y, z$; I: $1/2+x, -y, 3/4-z$).

Table 1 Crystal data for 1–4.

Compound	1	2	3	4
Empirical formula	C ₄₅ H ₅₅ O ₃₂ Sm ₃	C ₄₅ H ₅₅ Eu ₃ O ₃₅	C ₄₅ H ₅₅ O ₃₅ Tb ₃	C ₄₅ H ₅₅ Dy ₃ O ₃₅
Formula weight	1606.97	1611.77	1632.65	1643.39
Crystal system	Tetragonal	Tetragonal	Tetragonal	Tetragonal
Space group	<i>I</i> -4 ₂ d	<i>I</i> -4 ₂ d	<i>I</i> -4 ₂ d	<i>I</i> -4 ₂ d
<i>a</i> (Å)	14.3090(4)	14.2118(5)	14.1842(14)	14.1545(3)
<i>b</i> (Å)	14.3090(4)	14.2118(5)	14.1842(14)	14.1545(3)
<i>c</i> (Å)	63.900(4)	63.501(4)	63.709(9)	62.938(2)
<i>V</i> (Å ³)	13083.4(11)	12825.7(13)	12818(3)	12609.6(7)
<i>Z</i>	8	8	8	8
<i>D</i> _{calcd} (Mg/m ³)	1.632	1.669	1.692	1.731
μ (mm ⁻¹)	2.745	2.987	3.363	3.609
θ range (°)	3.120–26.419	3.141–25.678	3.124–26.726	2.950–25.878
Reflections collected	92596	71877	84991	89662
Data/Parameters	6688/322	5652/323	6562/333	6440/322
F(000)	6327	6352	6400	6424
<i>T</i> (K)	296.15	296.15	296.15	296.15
Flack	-0.0010(7)	0.09(4)	0.20(5)	-0.012(5)
<i>R</i> ₁ (<i>wR</i> ₂) [<i>I</i> > 2 σ (<i>I</i>)] ^a	0.0372 (0.0819)	0.0618 (0.1278)	0.0815 (0.1772)	0.0281 (0.0590)
Gof	1.064	1.069	1.087	1.114

$$^a R_1 = \frac{\sum ||F_o| - |F_c||}{\sum |F_o|}, wR_2 = \frac{[\sum w(F_o^2 - F_c^2)^2]}{\sum w(F_o^2)^2}]^{1/2}$$

**Figure 3.** Schematic view of the 3D frameworks with the 1D [Dy₃(COO)₉]_n chains along *b* direction.**Figure 4.** Unprecedented (3,8)-connected 3D (4.5²)₂(4².5¹².6⁶.7⁵.8³) net (green spheres: [Dy₃(COO)₆] SBUs; dark blue spheres: DDB⁴⁺ ligands).

Structure of {Ln_{1.5}(DDB)(FA)_{0.5}(H₂O)_{2.5}·6H₂O}_n (Ln = Sm for 1, Eu for 2, Tb for 3, and Dy for 4). Structural analyses reveal that complexes of 1–4 are isomorphism, and complex 4 is selected as a representative herein. Complex 4 crystallizes in tetragonal system, *I*-4₂d (122) space group. The asymmetric unit of 4 consists of one and a half of Dy(III) ions, one DDB⁴⁺ ligand, a half of FA⁻ anions, two and a half of coordinated water molecules, and six lattice water molecules. Dy(1) is nona-

coordinated with nine O atoms form four DDB⁴⁺ ligands and one coordinated water molecule. While Dy(2) is octa-coordinated by eight O atoms from three DDB⁴⁺ ligands, one FA⁻ anion, and two coordinated water molecules.

The H₄DDB ligand is completely deprotonated and twisted with the dihedral angles of 51.74(2)° and 62.09(1)° between two side phenyl rings and central phenyl ring, and 55.03(3)° between two side phenyl rings. DDB⁴⁺ acts as μ_5 node to coordinate with five Dy(III) ions with the carboxyl groups exhibit μ_2 - η^1 : η^1 , μ_1 - η^1 : η^1 , μ_2 - η^1 : η^2 , and μ_2 - η^1 : η^1 fashions (Fig. 1). Dy(III) ions are linked by carboxyl groups to form an unprecedented trinuclear [Dy₃(COO)₆] SBUs (Fig. 2) with the Dy...Dy distances being 4.127(1) Å for Dy(1)··Dy(2) and 7.852(7) Å for Dy(2)··Dy(2C). [Dy₃(COO)₆] SBUs were further expanded to form an interestingly 1D [Dy₃(COO)₉]_n chain *via in situ* generation of formate anion. Interestingly to note that those 1D chains expanded along different directions, finally interconnected by the DDB⁴⁺ ligands, leaving a high-symmetrically 3D framework with 1D oval void channels (Fig. 3). A PLATON program analysis suggests that there is approximately 37.0% of the crystal volume accessible to the solvent (4665.9 Å³ out of the 12609.6 Å³ unit cell volume).¹⁴ Hong group has been reported three *p*-terphenyl-3,3'',5,5''-tetracarboxylic acid based EuCPs, which showing different SBUs based 3D nets and 2D sheets.^{15a} While, when the hexacarboxylate ligand of *p*-terphenyl-2,2'',2''',5,5'',5'''-hexacarboxylate acid, and *p*-terphenyl-3,2'',3'',5,5'',5'''-hexacarboxylate acid were used to build LnCPs, the 3D pcu nets and 2D layers were obtained, respectively.^{15b} Compared this series with the above mentioned references, we can found that the backbones of the organic ligands play curial role in determining the structures as well as the porosity of the final architectures.

From the viewpoint of topology,¹⁶ the final 3D framework can be regard as a binodal (3,8)-connected net with the Schläfli Symbol of (4.5²)₂(4².5¹².6⁶.7⁵.8³) by simplifying the DDB⁴⁺ ligands and [Dy₃(COO)₆] SBUs as 3-connected and 8-connected nodes (Fig.4). From the perspective of modular design, the net was built from the tiling of 2{8b².8c}+{5b⁴}+2{4².5b².5d².8b²} with the transitivity of 2453 (Fig. 5).

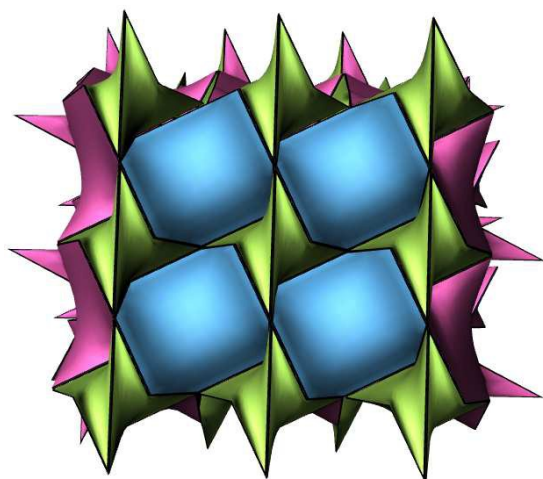


Figure 5. Tiling featured net of the 3D architecture.

Thermal Analyses. Thermogravimetric analysis (TGA) was performed on samples of **1–4** under N_2 with a heating rate of $5\ 10\ ^\circ C\ min^{-1}$, shown in Fig. S3. Due to that complexes **1–4** are isostructural, the four compounds exhibited similar thermal stability. The TGA curve displays mainly two steps of weight loss processes. The first weight loss of 19.6 % (calc. 19.0 %) for **1**, 19.7 % (calc. 19.0 %) for **2**, 18.7 % (calc. 18.7 %) for **3**, and 18.2 % (calc. 18.6 %) for **4** occurred below $175\ ^\circ C$ can be attributed to the loss of coordinated and lattice water molecules. Then the organic ligands begin to collapse due to thermal decomposition above to $410\ ^\circ C$.

Photoluminescent Investigation. The fluorescence spectrums of **1–4** and the free H_4DDB ligand were examined in the solid state at room temperature. As shown in the Fig. S4, the H_4DDB displays emission peak at $407\ nm$ upon excitation at $358\ nm$, which can be attributed to the $\pi^*-\pi$ transition of the p electrons of the aromatic rings.¹⁷ Complexes **1** and **4** exhibit broad and strong emissions that are centred at $393\ nm$ for **1** ($\lambda_{ex} = 308\ nm$), and $382\ nm$ for **4** ($\lambda_{ex} = 315\ nm$) (Fig. 6). The broad bands coincide with a ligand-based emission, indicating that the fluorescence of complexes **1** and **4** comes from the ligands.¹⁸ And the shoulder peaks around $470\ nm$ can be mainly attributed to the transitions of $^4G_{5/2} \rightarrow ^6H_{5/2}$ of Sm (III) ion for **1**, and $^4F_{9/2} \rightarrow ^6H_{15/2}$ of Dy (III) ion for **4**, respectively (Fig. 7). And the weak bands at $543\ nm$, $571\ nm$, and $621\ nm$ can be attributed to the transitions of $^4F_{9/2} \rightarrow ^6H_J$ of the Dy(III) ion with $J = 13/2$, $11/2$, and $9/2$, respectively.

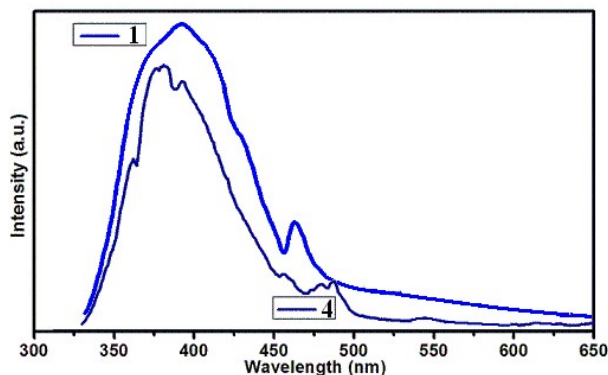


Figure 6. Emissionspectra of complexes **1** and **4** in the solid state at room temperature.

Table 2. Assignment of the energy transitions of the LnCPs.

Complex	Wavelength (nm)	Energy (cm^{-1})	transition
2	590	16949	$^5D_0 \rightarrow ^7F_1$
	613	16313	$^5D_0 \rightarrow ^7F_2$
	651	15361	$^5D_0 \rightarrow ^7F_3$
	699	14306	$^5D_0 \rightarrow ^7F_4$
3	488	20492	$^5D_4 \rightarrow ^7F_6$
	544	18382	$^5D_4 \rightarrow ^7F_5$
	584	17123	$^5D_4 \rightarrow ^7F_4$
	619	16155	$^5D_4 \rightarrow ^7F_3$

For complex **2**, under excitation at $395\ nm$, the emission spectrum of **2** exhibits sharp bands at 590 , 613 , 651 and $699\ nm$, which could be attributed to the transitions of $^5D_0 \rightarrow ^7F_J$ with $J = 1, 2, 3$, and 4 , respectively (Fig. 7). Two main characteristic peaks from $^5D_0 \rightarrow ^7F_2$ (red, $613\ nm$) and $^5D_0 \rightarrow ^7F_1$ (orange, $590\ nm$) are dominant. And the main energy level assignments of the titled complexes were listed in the Table 2. According to the international CIE standards, the CIE colour coordinates is $(0.65, 0.34)$ for **2**. The fluorescent intensity ratio for $^5D_0 \rightarrow ^7F_2$ to $^5D_0 \rightarrow ^7F_1$ transition reflects the inner structural information, such as the coordination environments of the Eu(III) ions in **2**. In addition, the intensity of $^5D_0 \rightarrow ^7F_2$ transition is much stronger than that of $^5D_0 \rightarrow ^7F_1$ transition.¹⁹

Under excitation at $315\ nm$, the emission spectrum of **3** exhibits sharp bands at 488 , 544 , 584 , and $619\ nm$, which correspond to the characteristic transitions of $^5D_4 \rightarrow ^7F_J$ of the Tb(III) ion with $J = 6, 5, 4$, and 3 , respectively (Fig. 7). The most intense emission at $544\ nm$ corresponds to the $^5D_4 \rightarrow ^7F_5$. Those above mentioned bands were assigned according to the energy level diagrams of Tb(III) ion.²⁰ And the CIE colour coordinates is $(0.29, 0.56)$ for **3**.

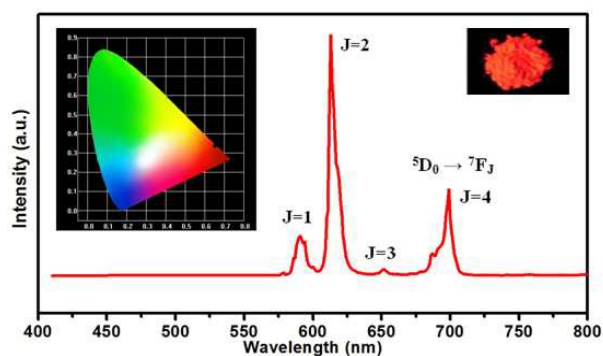


Figure 7. Emission spectrum of **2** under $395\ nm$ light. Inset: CIE chromaticity diagram and the fluorescent image of **2**.

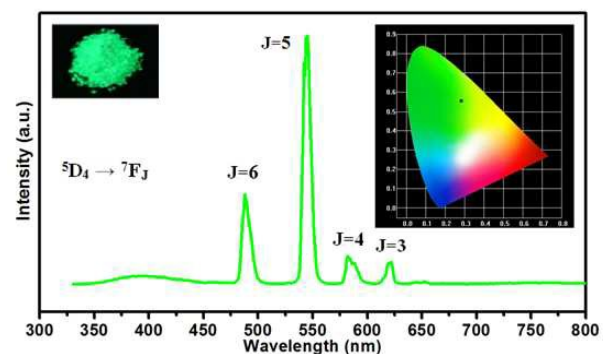


Figure 8. Emission spectrum of **3** under $315\ nm$ light. Inset: CIE chromaticity diagram and the fluorescent image of **3**.

As we all known, the tricolor combination (red, green, and blue) can show white light emission. Developing white light potential in general lighting applications is desirable. White light emission can be obtained by doping Dy(III) ions into the Eu(III) complex, because Dy(III) complexes display blue light emission, which is the complementary color of red emission from the Eu(III) ion. These Ln(III) ions have both similar ionic radii and coordination geometries. The synthetic method is same as that mentioned above just by loading the corresponding Ln(NO₃)₃·6H₂O as the starting materials in stoichiometric ratios. Thus, Eu(III) was doped separately into the Dy(III) complex, and generation of Dy_xEu_{1-x} doped complexes is attempted, the powder X-ray diffractions were also were measured to identify the doped complexes are isomorphism with the single component complexes (Fig. S4). The emission spectra of Dy_{0.9}Eu_{0.1}, Dy_{0.8}Eu_{0.2}, Dy_{0.7}Eu_{0.3}, Dy_{0.6}Eu_{0.4}, and Dy_{0.5}Eu_{0.5} doped materials are similar (Fig. 9). And the sharp main emission peaks at 591 and 613 nm are attributed to transitions of ⁵D₀ → ⁷F_J (J = 1, 2) of the Eu(III) ion and the broad emission band in the region of 420–500 nm is from the ligand. When those doped materials are excited at 390 nm, the CIE coordinates (0.31, 0.28), (0.33, 0.31), (0.35, 0.32), (0.37, 0.33), and (0.45, 0.34) for Dy_{0.9}Eu_{0.1}, Dy_{0.8}Eu_{0.2}, Dy_{0.7}Eu_{0.3}, Dy_{0.6}Eu_{0.4}, and Dy_{0.5}Eu_{0.5} doped complexes, respectively. And the Dy_{0.8}Eu_{0.2} as well as Dy_{0.7}Eu_{0.3} doped complexes are closed with the CIE coordinates of the standard white light (0.33, 0.33), according to the CIE 1931 coordinate diagram. Consequently, white light emission is achieved by Dy–Eu doped complexes under the broad UV region.²¹

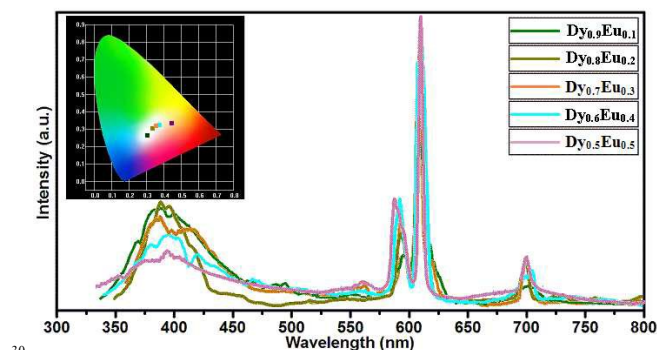


Figure 9. Emission spectra of Dy_xEu_{1-x} doped complexes with $\lambda_{\text{exc}} = 390$ nm. Inset: CIE chromaticity diagram.

Conclusions

In summary, series isomorphous LnCPs have been hydrothermally synthesized and characterized based on the W-shaped 1,3-di(2,4-dicarboxyphenyl)benzene. Complexes **1–4** exhibit unique (3,8)-connected 3D architecture with the Point Schläfli Symbol of (4.5²)₂(4².5¹².6⁶.7⁵.8³), based on the trinuclear [Ln₃(COO)₆] SBUs. Besides, solid state luminescence investigation indicated that **1** and **4** show ligand-based emission, while **2** and **3** display characteristic red and green light emissions, respectively. White light emission can be achieved by doping the Eu(III) ions into the Dy(III) complexes. Further work of LnCPs based on polycarboxylate ligands are underway in our lab.

Acknowledgements. The work was supported by financial support from the Natural Science Foundation of China (Grant Nos. 21101097, 21451001), key discipline and innovation team of Qilu Normal University.

Notes

The authors declare no competing financial interest.

References

- (a) J. Rocha, L. D. Carlos, F. A. Almeida Paz and D. Ananias, *Chem. Soc. Rev.*, 2011, **40**, 926; (b) Y. Cui, Y. Yue, G. Qian and B. Chen, *Chem. Rev.*, 2012, **112**, 1126; (c) W. Xu, Y. Zhou, D. Huang, M. Su, K. Wang, and M. Hong, *Inorg. Chem.*, 2014, **53**, 6497; (d) Y. Cui, B. Chen and G. Qian, *Coord. Chem. Rev.*, 2014, **273–274**, 76; (e) X. Zhao, M. Wong, C. Mao, T. X. Trieu, J. Zhang, P. Feng and X. Bu, *J. Am. Chem. Soc.*, 2014, **136**, 12572; (f) S. D. Bennett, B. A. Core, M. P. Blake, S. J. A. Pope, P. Mountford and B. D. Ward, *Dalton Trans.*, 2014, **43**, 5871.
- (a) D. N. Woodruff, R. E. P. Wimpenny, and R. A. Layfield, *Chem. Rev.*, 2013, **113**, 5110; (b) K. Binnemans, *Chem. Rev.*, 2009, **109**, 4283; (c) Y. –T. Liang, G. –P. Yang, B. Liu, Y. –T. Yan, Z. –P. Xi and Y. –Y. Wang, *Dalton Trans.*, 2015, **44**, 13325; (d) K. Miyata, Y. Konno, T. Nakanishi, A. Kobayashi, M. Kato, K. Fushimi and Y. Hasegawa, *Angew. Chem. Int. Edit.*, 2013, **52**, 6413; (e) Z. –C. Yue, H. –J. Du, Y. –Y. Niu and G. –X. Jin, *CrystEngComm*, 2013, **15**, 9844; (f) L. M. A. Saleh, K. H. Birj Kumar, A. V. Protchenko, A. D. Schwarz, S. Aldridge, C. Jones, N. Kaltsoyannis, and P. Mountford, *J. Am. Chem. Soc.*, 2011, **133**, 3836.
- (a) Z. Hu, B. J. Deibert and J. Li, *Chem. Soc. Rev.*, 2014, **43**, 5815; (b) K. Binnemans, *Chem. Rev.*, 2009, **109**, 4283; (c) H. He, H. Ma, D. Sun, L. Zhang, R. Wang, and D. Sun, *Cryst. Growth Des.*, 2013, **13**, 3154; (d) X. Yang, R. A. Jones and S. Huang, *Coord. Chem. Rev.*, 2014, **273–274**, 63; (e) X. Liu, S. Akerboom, M. d. Jong, I. Mutikainen, S. Tanase, A. Meijerink, and E. Bouwman, *Inorg. Chem.*, 2015, **54**, 11323; (f) F. Bu, Q. Lin, Q. –G. Zhai, X. Bu and P. Feng, *Dalton Trans.*, 2015, **44**, 16671; (g) G. Cosquer, M. Morimoto, M. Irie, A. Fetoh, B. K. Breedlove and M. Yamashita, *Dalton Trans.*, 2015, **44**, 5996.
- (a) K. Su, F. Jiang, J. Qian, L. Chen, J. Pang, S. M. Bawaked, M. Mokhtar, S. A. Al-Thabaiti, and M. Hong, *Inorg. Chem.*, 2015, **54**, 3183; (b) X. Zhang, L. Fan, W. Fan, B. Li and X. Zhao, *CrystEngComm*, 2015, **17**, 6681; (c) J. Ma, F. –L. Jiang, L. Chen, M. –Y. Wu, S. –Q. Zhang, K. Xiong, D. Han and M. –C. Hong, *CrystEngComm*, 2012, **14**, 6055; (d) X. Feng, R. Li, L. Wang, S. W. Ng, G. Qin and L. M., *CrystEngComm*, 2015, **17**, 7878; (e) K. Katoh, Y. Horii, N. Yasuda, W. Wernsdorfer, K. Toriumi, B. K. Breedlove and M. Yamashita, *Dalton Trans.*, 2012, **41**, 13582; (f) W. Cao, H. Wang, X. Wang, H. K. Lee, D. K. P. Ng and J. Jiang, *Inorg. Chem.*, 2012, **51**, 9265.
- (a) X. Feng, Y. –Q. Feng, J. J. Chen, S. –W. Ng, L. –Y. Wang and J. –Z. Guo, *Dalton Trans.*, 2015, **44**, 804; (b) N. C. Anastasiadis, D. A. Kalofolias, A. Philippidis, S. Tzani, C. P. Raptopoulou, V. Psycharis, C. J. Milios, A. Escuer and S. P. Perlepes, *Dalton Trans.*, 2015, **44**, 10200; (c) X. Feng, L. –Y. Wang, J. –G. Wang, C. –Z. Xie, J. –S. Zhao and Q. Sun, *CrystEngComm*, 2010, **12**, 3476; (d) X. Feng, S. –H. Li, L. –Y. Wang, J. –S. Zhao, Z. –Q. Shi and P. –P. Lei, *CrystEngComm*, 2012, **14**, 3684; (e) X. –T. Zhang, L. –M. Fan, W. –L. Fan, B. Li, G. –Z. Liu, X. –Z. Liu and X. Zhao, *Cryst. Growth Des.*, 2016, **DOI**: 10.1021/acs.cgd.6b00540.
- (a) C. Marchal, Y. Filinchuk, X. –Y. Chen, D. Imbert and M. Mazzanti, *Chem-Eur. J.*, 2009, **15**, 5273; (b) J. Zhao, G. –H. Zhu, L. –Q. Xie, Y. –S. Wu, H. –L. Wu, A. –J. Zhou, Z. –Y. Wu, J. Wang, Y. –C. Chen and M. –L. Tong, *Dalton Trans.*, 2015, **44**, 14424; (c) D. –S. Li, Y. –P. Wu, J. Zhao, J. Zhang, J. Y. Lu, *Coord. Chem. Rev.*, 2014, **261**, 1; (d) K. Katoh, R. Asano, A. Miura, Y. Horii, T. Morita, B. K. Breedlove and M. Yamashita, *Dalton Trans.*, 2014, **43**, 7716; (e) X. Zhao, M. Wong, C. Mao, T. X. Trieu, J. Zhang, P. Feng, and X. Bu, *J. Am. Chem. Soc.*, 2014, **136**, 12572.

7. (a) Z. J. Lin, J. Lü, M. Hong and R. Cao, *Chem. Soc. Rev.*, 2014, **43**, 5867; (b) F. A. A. Paz, J. Klinowski, S. M. F. Vilela, J. P. C. Tomé, J. A. S. Cavaleiro and J. Rocha, *Chem. Soc. Rev.*, 2012, **41**, 1088; (c) Y. Gai, F. Jiang, L. Chen, M. Wu, K. Su, J. Pan, X. Wan, and M. Hong, *Cryst. Growth Des.*, 2014, **14**, 1010; (d) Q. –G. Zhai, N. Bai, S. Li, X. Bu and P. Feng, *Inorg. Chem.*, 2015, **54**, 9862; (e) X. Feng, X. –L. Ling, L. Liu, H. –L. Song, L. –Y. Wang, S. –W. Ng and B. Y. Su, *Dalton Trans.*, 2013, **42**, 10292.
8. (a) Y. He, B. Li, M. O’Keeffe and B. Chen, *Chem. Soc. Rev.*, 2014, **43**, 5618; (b) F. Dai, P. Cui, F. Ye and D. Sun, *Cryst. Growth Des.*, 2010, **10**, 1474; (c) X. Feng, Y. –Q. Feng, L. Liu, L. –Y. Wang, H. –L. Song and S. –W. Ng, *Dalton Trans.*, 2013, **42**, 7741; (d) X. Zhang, L. Fan, Z. Sun, W. Zhang, W. Fan, L. Sun and X. Zhao, *CrystEngComm*, 2013, **15**, 4910.
9. (a) R. Huo, X. Li and D. Ma, *CrystEngComm*, 2015, **17**, 3838; (b) X. Ma, X. Li, Y. –E. Cha, and L. –P. Jin, *Cryst. Growth Des.*, 2012, **12**, 5227; (c) Y. –H. Zhang, X. Li, S. Song, H. –Y. Yang, D. Ma and Y. –H. Liu, *CrystEngComm*, 2014, **16**, 8390; (d) S. Song, X. Li, Y. –H. Zhang, R. Huo and D. Ma, *Dalton Trans.*, 2014, **43**, 5974.
10. (a) P. R. Matthes, C. J. Höller, M. Mai, J. Heck, S. J. Sedlmaier, S. Schmiechen, C. Feldmann, W. Schnick, K. Müller–Buschbaum, *J. Mater. Chem.*, 2012, **22**, 10179; (b) D. Ma, X. Li and R. Huo, *J. Mater. Chem. C*, 2014, **2**, 9073; (c) H. L. Guo, Y. Z. Zhu, S. L. Qiu, J. A. Lercher, H. J. Zhang, *Adv. Mater.*, 2010, **22**, 4190; (d) K. Liu, H. P. You, Y. H. Zheng, G. Jia, Y. H. Song, Y. J. Huang, M. Yang, J. J. Jia, N. Guo, H. J. Zhang, *J. Mater. Chem.*, 2010, **20**, 3272.
11. (a) L. Fan, W. Fan, W. Song, G. Liu, X. Zhang and X. Zhao, *CrystEngComm*, 2014, **16**, 9191; (b) X. Zhang, L. Fan, W. Fan and X. Zhao, *Z. Anorg. Allg. Chem.*, 2015, **641**, 1808; (c) L. Fan, W. Fan, B. Li, X. Zhao and X. Zhang, *RSC Adv.*, 2015, **5**, 39854.
12. (a) G. M. Sheldrick, *SHELXTL*, version 5.1; Bruker Analytical X-ray Instruments Inc.: Madison, WI, 1998. (b) G. M. Sheldrick, *SHELX-97*, PC Version; University of Gottingen: Gottingen, Germany, 1997.
13. (a) L. Fan, X. Zhang, W. Zhang, Y. Ding, W. Fan, L. Sun and X. Zhao, *CrystEngComm*, 2014, **16**, 2144; (b) X. Zhang, L. Fan, Z. Sun, W. Zhang, D. Li, J. Dou and L. Han, *Cryst. Growth Des.*, 2013, **13**, 792; (c) L. Fan, X. Zhang, Z. Sun, W. Zhang, Y. Ding, W. Fan, L. Sun, X. Zhao, and H. Lei, *Cryst. Growth Des.*, 2013, **13**, 2462.
14. (a) A. L. Spek, *J. Appl. Crystallogr.*, 2003, **36**, 7; (b) A. L. Spek, *PLATON, A Multipurpose Crystallographic Tool*, Utrecht University, Utrecht, The Netherlands, 2002.
15. (a) Y. –L. Gai, F. –L. Jiang, L. Chen, Y. Bu, K. –Z. Su, S. A. Al-Thabaiti and M. –C. Hong, *Inorg. Chem.*, 2013, **52**, 7658; (b) Y. Gai, F. Jiang, L. Chen, M. Wu, K. Su, J. Pan, X. Wan and M. Hong, *Cryst. Growth Des.*, 2014, **14**, 1010.
16. (a) V. A. Blatov, A. P. Shevchenko and V. N. Serezhkin, *J. Appl. Crystallogr.*, 2000, **33**, 1193; (b) The network topology was evaluated by the program “TOPOS-4.0”, see: <http://www.topos.ssu.samara.ru>. (c) V. A. Blatov, M. O’Keeffe and D. M. Proserpio, *CrystEngComm*, 2010, **12**, 44; (d) V. A. Blatov, M. O’Keeffe and D. M. Proserpio, *CrystEngComm*, 2010, **10**, 44.
17. (a) L. Fan, W. Fan, B. Li, X. Zhao and X. Zhang, *CrystEngComm*, 2015, **17**, 9413; (b) D. Sun, F. J. Liu, H. J. Hao, Y. H. Li, N. Zhang, R. B. Huang and L. S. Zheng, *CrystEngComm*, 2011, **13**, 5661; (c) L. Fan, W. Fan, B. Li, X. Liu, X. Zhao and X. Zhang, *RSC Adv.*, 2015, **5**, 14897; (d) X. Zhang, L. Fan, W. Zhang, W. Fan, L. Sun and X. Zhao, *CrystEngComm*, 2014, **16**, 3203; (e) L. –L. Liu, C. –X. Yu, Y. –R. Li, J. –J. Han, F. –J. Ma and L. –F. Ma, *CrystEngComm*, 2015, **17**, 653; (f) D. –S. Liu, Y. Sui, W. –T. Chen and P. Feng, *Cryst. Growth Des.*, 2015, **15**, 4020.
18. (a) L. –L. Han, T. –P. Hu, K. Mei, Z. –M. Guo, C. Yin, Y. –X. Wang, J. Zheng, X. –P. Wang and D. Sun, *Dalton Trans.*, 2015, **44**, 6052; (b) L. Fan, W. Fan, B. Li, X. Liu, X. Zhao and X. Zhang, *Dalton Trans.*, 2015, **44**, 2380; (c) X. Zhang, L. Fan, W. Song, W. Fan, L. Sun and X. Zhao, *RSC Adv.*, 2014, **4**, 30274; (d) L. –L. Liu, C. –X. Yu, F. –J. Ma, Y. –R. Li, J. –J. Han, L. Lin and L. –F. Ma, *Dalton Trans.*, 2015, **44**, 1636; (e) G. –W. Xu, Y. –P. Wu, H. –B. Wang, Y. –N. Wang, D. –S. Li and Y. –L. Liu, *CrystEngComm*, 2015, **17**, 9055; (f) Q. Lin, X. Bu, C. Mao, X. Zhao, K. Sasan and P. Feng, *J. Am. Chem. Soc.*, 2015, **137**, 6184.
19. (a) J. Jia, J. Xu, S. Wang, P. Wang, L. Gao, M. Yu, Y. Fan and L. Wang, *CrystEngComm*, 2015, **17**, 6030; (b) L. Zhai, W. –W. Zhang, X. –M. Ren and J. –L. Zuo, *Dalton Trans.*, 2015, **44**, 5746; (c) Q. Li and S. Du, *RSC Adv.*, 2014, **4**, 30963; (d) L. Zhang, H. Zhu, Y. Guo, Y. Zhou, Q. Yue and Z. Shi, *CrystEngComm*, 2015, **17**, 4150; (e) Y. Yang, F. Jiang, C. Liu, L. Chen, Y. Gai, J. Pang, K. Su, X. Wan and M. Hong, *Cryst. Growth Des.*, 2016, **16**, 2266.
20. (a) W. Wang, J. Yang, R. Wang, L. Zhang, J. Yu, and D. Sun, *Cryst. Growth Des.*, 2015, **15**, 2589; (b) D. K. Singha, P. Majee, S. K. Mondal and P. Mahata, *RSC Adv.*, 2015, **5**, 102076; (c) Q. Li and S. Du, *RSC Adv.*, 2015, **5**, 9898; (d) X. Feng, J. –L. Chen, L. –Y. Wang, S. –Y. Xie, S. Yang, S. –Z. Huo and S. –W. Ng, *CrystEngComm*, 2014, **16**, 1334; (e) H. Wang, D. Zhang, Z. –H. Ni, X. Li, L. Tian and J. Jiang, *Inorg. Chem.*, 2009, **48**, 5946.
21. (a) S. Dang, J. –H. Zhang, Z. –M. Sun, *J. Mater. Chem.*, 2012, **22**, 8868; (b) D. Ma, R. Huo and X. Li, *CrystEngComm*, 2015, **17**, 6575; (c) Q. –Y. Yang, M. Pan, S. –C. Wei, K. Li, B. –B. Du, and C. –Y. Su, *Inorg. Chem.*, 2015, **54**, 5707; (d) L. Zhang, Z. Kang, X. Xin and D. Sun, *CrystEngComm*, 2016, **18**, 192.

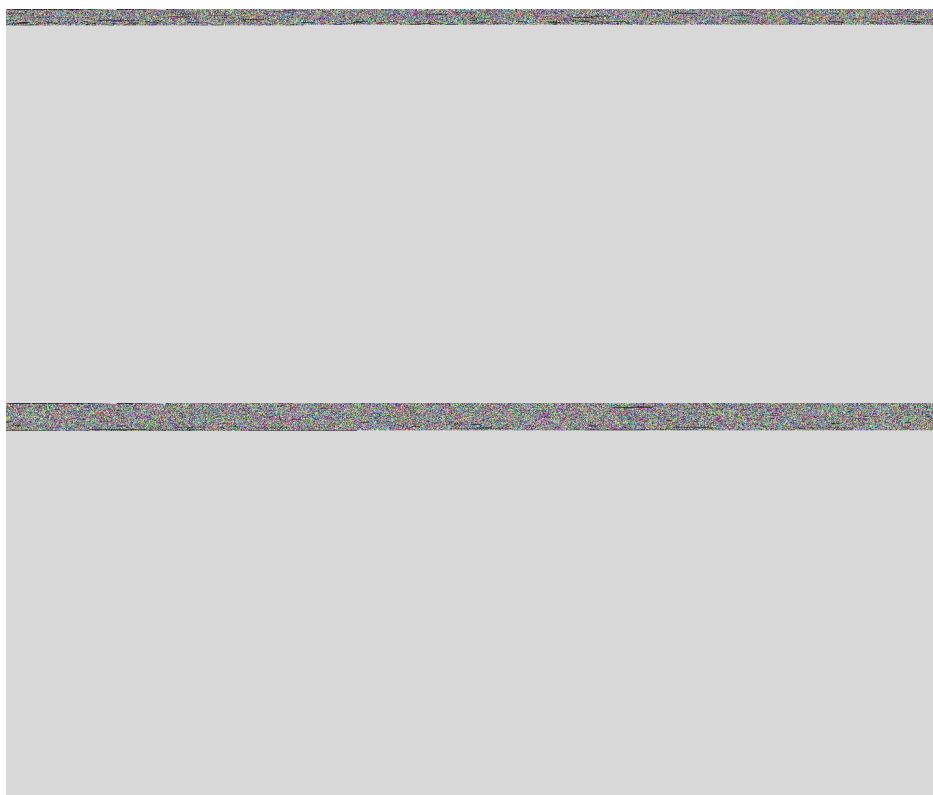
New Journal of Chemistry

For Table of Contents Use Only

Table of Contents Graphic and Synopsis**W-shaped 1,3-Di(2,4-dicarboxyphenyl)benzene Based Lanthanide
5 Coordination Polymers with Tunable White Light Emission**

Liming Fan (L. Fan), Weiliu Fan (W. Fan), Bin Li (B. Li), Xiutang Zhang (X. Zhang), and Xian Zhao (X. Zhao)

Series trinuclear LnCPs with unprecedented (3,8)-connected 3D $(4.5^2)_2(4^2.5^{12}.6^6.7^5.8^3)$ architectures were synthesized. White light emissions were realized by the Eu(III)-doped Dy(III) complexes.



10